Propagation of short-wavelength electromagnetic surface waves along the transition layer between two plasma-like half-spaces in the Voigt geometry

Igor O. Girka[1,2], Manfred Thumm[3]

1 - V.N.Karazin Kharkiv National University, Svobody sq., 4, 61022, Kharkiv, Ukraine. (e-mail: igorgirka@karazin.ua).

2 – Max-Planck-Institut für Plasmaphysik, Boltzmannstr. 2, 85748, Garching, Germany

3 – Karlsruhe Institute of Technology, IHM and IHE, 76131, Karlsruhe, Germany

Abstract – The dispersion properties of surface type electromagnetic waves are studied. The waves are considered to propagate along a slab transition layer located between two infinite homogeneous plasma regions of different particle densities. The wavelength is assumed to be short as compared with the layer width. The waves propagate across a static magnetic field which is parallel to the layer interface. The influence of the smoothness of the gradient of the plasma particle density within the layer on the surface wave propagation/disappearance is discussed. The conclusions derived in the present paper are of interest in the fields of plasma electronics, nano-technologies, plasma-antenna systems, plasma production, and magnetic confinement fusion.

Key words: surface electromagnetic waves, Voigt geometry, static magnetic field, plasma-plasma interface, transition layer, plasma particle density smoothness

I. Introduction

Real plasmas do not have absolutely sharp boundaries. An interface between the plasma and another medium can be considered as a sharp one in studies of

electromagnetic Surface Wave (SW) propagation only if the width of the transition layer is much smaller than the wave penetration depth. This takes place in particular at the interfaces of plasmas in semiconductors. The model of sharp boundary was effectively applied as first approach in many studies in the past.

Interest to SW propagation and excitation is explained by their extensive application in many fields of physics and technology (see e.g. [1] and references therein). Specifically, SWs play an important role in plasma electronics [2,3] since they propagate within those frequency ranges where bulk waves do not propagate. Surface-enhanced Raman scattering demonstrates its potential in various types of ultrasensitive sensing applications in a wide variety of fields [4]. In recent years, SWs have obtained a new field of application, namely plasma-antenna systems. These plasma antennas get advantage from utilization of a plasma as medium with sufficiently high conductivity instead of metal wires which makes it possible to be quickly switched-off and/or switched-on [5]. Radio frequency (RF) gas discharges sustained by SWs appear to be very convenient for plasma production since they are generally less expensive, easier to handle, more efficient, and more reliable sources of particles and radiation as compared with the various DC discharges [6]. RF power was mentioned in [7] to be lost during RF wave penetration through the plasma periphery in magnetic confinement thermonuclear fusion plasma devices, because of parasitic absorption. In particular, undesirable excitation of SWs by RF antennas was reported in [8] to be foreseen in the plasma periphery of DEMO and ITER. Further optimization which could help to avoid excitation of these SWs was also discussed. However, the considered model was in a slab geometry only.

Interest to the role of the transition layer between two plasma layers is often explained by the presence of local resonances therein, which can cause in particular additional plasma heating. Since in most cases the transition layer separates the plasma layer from vacuum, the heating can take place in the plasma edge. The latter

can be a parasitic phenomenon if one has the objective to heat the plasma core, like it happens in controlled thermonuclear fusion devices with magnetic plasma confinement. On the other hand, edge plasma heating can be of interest for technological applications if one has the goal to process the surface of a sample with plasma-like properties.

In the case of isotropic plasmas, modelling the plasma density within the transition layer by using a linear dependence makes it possible to reduce the Laplace equation to a second order differential equation of Bessel type. An analytic expression for the damping rate of surface waves caused by the presence of a local resonance in the transition layer at the plasma edge was derived in [9]. The damping rate was shown to be independent of the collision frequency. The dispersion relation was demonstrated to have no solution if the transition layer width was larger than the wavelength. This was treated as the disappearance of the SWs.

Electromagnetic energy absorption within the local plasma resonance in the transition layer at the edge of isotropic plasmas was carefully studied in [10]. Three structures were considered: flat boundary vacuum-plasma, thin flat layer, and thin plasma cylinder.

The influence of the viscosity on the resonance absorption of incompressible magnetohydrodynamic SWs within a thin transition layer was considered in [11]. The classical viscous stress tensor for a magnetized plasma was applied. The electromagnetic power absorption was evaluated and found to be independent of the viscosity coefficient, and to correspond to SW power absorption obtained from the equations of ideal magnetohydrodynamics.

The growth rate of SWs in the presence of a p-polarized pump wave (electric field is polarized parallel to the plane of incidence) was reported in [12] to be by several orders of magnitude larger as compared with that in the case of sharply bounded plasmas. The mechanism of this process was explained as follows. The

plasmons localized in the plasma vacuum transition layer were shown to be parametrically excited and transfer their energy to the surface waves. The width of the transition layer was assumed to be small as compared to the wavelengths involved in the problem and large as compared to the Debye length of the electrons.

The presence of local resonances can result in the higher importance of nonlinear phenomena occurring in the boundary region than those of the bulk plasma. The nonlinear phenomena were noted in [13] to cause a significant modification of the SW dispersion relations derived under assumption of a sharp boundary.

The propagation of electromagnetic SWs with account for nonlinear phenomena inside a diffuse boundary was considered in [14]. The plasma particle density profile within the transition layer was assumed to be linear. The width of the layer was suggested to be smaller than the wavelength of the surface wave and larger than the electron Debye length. An external static magnetic field was neglected.

A variety of experimental techniques which provide indirect evidence of the existence of local resonances in a transition layer was noted, e.g., in [15] for plasma discharges with various configurations and dimensions sustained by SWs. A review of experiments and discussions about the existence of such resonances can be found in [16].

The authors of the present study also contributed to the analysis of electromagnetic energy absorption within local resonances [see, e.g., 17-19]. However, even the brief overview of the role of local resonances presented above makes it possible to conclude that the role is clarified well enough. The main motivation for the present study is to assess the effect of the transition layer on SW propagation for the case that no resonances are influencing the SWs. This might be important, because in many numerical cases SWs can appear close to resonances, and it is not clear what the reason for SWs is: the discontinuity of the medium or the

resonance itself. That is why the present paper deals with transition layers without any local resonance.

The dispersion properties of SWs propagating along the interface of a metal and a semibounded gaseous plasma in Voigt geometry were analyzed in [20] with account for plasma particle density inhomogeneity in the direction perpendicular to the interface. The non-uniformity was modeled by introducing a transition layer where the density varied according to a three-parameter sinusoidal law. Lack of computing possibilities did not allow the authors to make an in-depth analysis of the influence of the transition layer parameters on the wave dispersion properties. The main conclusion was about the tangential component of the SW electric field. Its amplitude was reported to be non-zero inside the plasma and to be zero at the plasma-metal interface in contrast to the case of the sharp boundary between the metal and uniform plasma, for which the tangential component of the SW electric field is equal to zero inside the entire plasma. The qualitative conclusion about the dependence of the wave eigenfrequency on the plasma density sharpness within the transition layer was in agreement with the wave dispersion properties in a uniform plasma half-space. An overview of these results can be found in [21].

The metal wall was naturally modelled in [21] as ideal (non-dissipative) medium with infinite plasma particle density. The main distinguishing feature of the present study, compared to that in [21], is that the metal in the left half space is replaced by a plasma with finite density.

The present study was initiated by the following motivation. Often, an inhomogeneous plasma density profile is modelled by a set of radial layers of different widths and steps of uniform density. For instance, in numerical calculations, sharp plasma–vacuum interfaces are commonly used as a simple method of avoiding issues associated with local resonances. However, additional roots of the dispersion relation are the unavoidable consequence of introducing

additional interfaces between plasma layers of different densities. These non-physical SWs also prevent convergence in numerical calculations within the ion cyclotron frequency range [22].

The paper is arranged as follows. The motivation of the study is explained in Introduction being section I. The model to be considered is reported in section II. Short explanation of how the wave equation is derived is provided in section III. Wave field spatial distributions in the left half space, right half space and within the transition layer are given in sections IV, V, and VI respectively. The dispersion relation is derived and analytically investigated in section VII. The results of numerical studying the SW dispersion properties are presented in section VIII. The main conclusions and discussions are displayed in section IX.

II. Model description

The following plasma structure is considered (Fig. 1). The half space $x < -a/2$ is occupied by uniform cold collisionless plasma with the plasma particle density n_1. A plasma with another uniform particle density $n_3 > n_1$ is placed in the half space $x > a/2$. A transition plasma layer of the width a separates the half

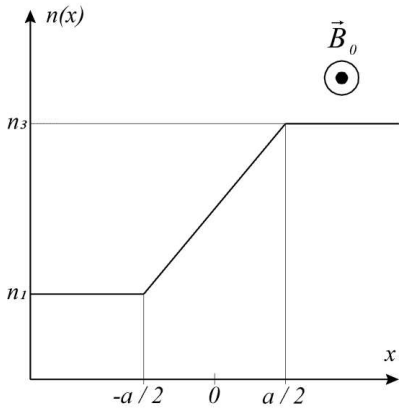

Fig. 1. Schematic of the problem. Left: uniform plasma half space: $x < -a/2$, transition layer: $-\frac{a}{2} < x < a/2$, right: uniform plasma half space: $x > a/2$

spaces with uniform, but different plasma particle densities. An external static magnetic field $\vec{B}_0$ is assumed to be parallel to the interfaces between the three media. Its direction is chosen to coincide with the axis $\vec{z}$, $\vec{B}_0 || \vec{z}$.

One can choose the position of the transition layer in any other way. For example, one plasma medium can be placed in the half space $x < b \neq -a/2$, and the other in the half space $x > b + a$ with b being an arbitrary constant. Such approach with $b = 0$ was realized, e.g. in [1,20]. However, it is demonstrated below that it is the position $b = -a/2$ chosen in the present paper, which provides the symmetry of the problem, which in its turn simplifies algebra and makes the solution self-consistent. The symmetry means that the considered structure coincides with itself in the result of a coordinate system rotation around the z axis by the angle of π with the only consequence that plasma particle density gradient becomes negative. Plasma electrodynamic properties are described in terms of the cold collisionless plasma tensor of dielectric permittivity ε_{ij}:

$$\hat{\varepsilon} = \begin{pmatrix} \varepsilon_1 & i\varepsilon_2 & 0 \\ -i\varepsilon_2 & \varepsilon_1 & 0 \\ 0 & 0 & \varepsilon_3 \end{pmatrix}. \quad (1)$$

The components of the tensor read

$$\varepsilon_1 = 1 - \sum_\alpha \frac{\Omega_\alpha^2}{\omega^2 - \omega_\alpha^2},\ \varepsilon_2 = -\sum_\alpha \frac{\Omega_\alpha^2 \omega_\alpha}{\omega(\omega^2 - \omega_\alpha^2)},\ \varepsilon_3 = 1 - \sum_\alpha \frac{\Omega_\alpha^2}{\omega^2}. \quad (2)$$

In (2), Ω_α is the plasma frequency of the particle of species α ($\alpha = i$ for ions and $\alpha = e$ for electrons), ω_α is corresponding cyclotron frequency.

III. Wave equation

The present study is restricted to consideration of transversal (whose wave vector is perpendicular to the external static magnetic field, $k_z = 0$) electromagnetic

waves of extraordinary polarization (with the wave field components E_x, E_y, H_z). The temporal-spatial dependence of the wave longitudinal magnetic field reads

$$H_z(\vec{r}, t) = H_z(x)\exp\left[i(k_y y - \omega t)\right]. \quad (3)$$

In (3), k_y and ω are the wavenumber in y-direction and the wave angular frequency, respectively.

This configuration, in which the waves propagate across the external static magnetic field, which in turn is parallel to the interface, is known to be called as Voigt geometry [21]. The theory of surface electromagnetic wave propagation in Voigt geometry along the plasma-metal interface in plane and circular (partially) waveguides was overviewed in [21]. A comprehensive review of SW propagation, beam excitation and applications in circular waveguides was given in [1]. Note that transversal electromagnetic surface waves of ordinary polarization (with the wave field components H_x, H_y, E_z) do not propagate in the plasma structure considered here, for any magnitude of the wavenumber k_y. The restriction to set the axial wavenumber equal to zero ($k_z = 0$) makes the problem tractable. In addition, application of such simplification is justified by the following reason. The authors of [23] considered SW propagation at an arbitrary angle to $\vec{B}_0$ along the slab plasma-metal interface. They concluded that the wave field components H_x, H_y, E_z are not negligible only in a small region of the phase plane (k_y, k_z).

Maxwell equations provide the following second order uniform differential equation for the amplitude $H_z(x)$ of the longitudinal magnetic wave field

$$\frac{d}{dx}\left(\frac{1}{k_\perp^2}\frac{dH_z}{dx}\right) - H_z\left[1 + \frac{k_y^2}{k_\perp^2} - \frac{d}{dx}\left(\frac{\mu k_y}{k_\perp^2}\right)\right] = 0. \quad (4)$$

In (4), $k_\perp^2 = k^2 N_\perp^2, N_\perp^2 = \varepsilon_1(\mu^2 - 1) > 0, \mu = \varepsilon_2/\varepsilon_1, k = \omega/c$. If the plasma is uniform, eq. (4) reads:

$$\frac{d^2H_z}{dx^2} - \left[k_\perp^2 + k_y^2\right]H_z = 0. \quad (5)$$

IV. Wave field distribution in the left half space

In the left half space, $x < -a/2$, the solution of eq. (5) which has the form of a surface wave and meets the boundary condition at $x \to -\infty$ reads

$$H_z^{(1)}(x) = A\exp[k_1(x + a/2)], \quad (6)$$

$$E_y^{(1)}(x) = \frac{i}{N_{\perp 1}^2} A\,(\mathrm{N}_1 + \mu_1 \mathrm{N}_y)\exp[k_1(x + a/2)]. \quad (7)$$

In (6) and (7), A is the constant of integration, $N_y = k_y/k$ is refractive index, and $N_{1,3} = k_{1,3}/k$. The depth k_1^{-1} of wave penetration into the plasma in this region is determined as $k_{1,3}^2 = k_{\perp 1,3}^2 + k_y^2$ for the plasma particle density $n = n_1$. The subscript "1" nearby the observables μ_1, and $N_{\perp 1}^2$ means that they are calculated for $n = n_1$.

V. Wave field distribution in the right uniform half space

In the right uniform region, $x > a/2$, the solution of the Maxwell equations, which has the form of a surface wave and satisfies the boundary condition at $x \to +\infty$, reads

$$H_z^{(3)}(x) = B\exp[-k_3(x - a/2)], \quad (8)$$

$$E_y^{(3)}(x) = \frac{i}{N_{\perp 3}^2} B\,(-\mathrm{N}_3 + \mu_3 \mathrm{N}_y)\exp[-k_3(x - a/2)]. \quad (9)$$

In (8) and (9), B is the constant of integration, μ_3 and $N_{\perp 3}^2$ are the observables μ and $N_\perp^2$ calculated for higher plasma particle density, $n = n_3$.

VI. Wave field distribution in the transition layer

In the following, only short wavelength waves are under the consideration. This means that the wave length is assumed to be sufficiently small:

$$|k_y| \gg |k_{\perp 1,3}|, 1/a. \tag{10}$$

Note that the condition $k_y^2 > |k_{\perp 1,3}^2|$ is necessary to provide surface nature of the wave in the uniform half-spaces if $k_{\perp 1,3}^2$ is negative. The strong inequality (10) can also be treated as sufficiently large width of the transition layer which excludes the possibility to use the results of studying SWs propagation along a sharp plasma-plasma interface as a limiting case.

Then asymptotic methods can be applied for solving eq. (4) within the transition layer, $-a/2 < x < a/2$. In particular, the amplitude of the magnetic wave field can be presented as the series $H_z^{(2)} = H_z^{(2,0)} + H_z^{(2,1)}$ ($|H_z^{(2,1)}| \ll |H_z^{(2,0)}|$) where the main term $H_z^{(2,0)}$ is the solution to eq. (4) in zero approximation:

$$\frac{1}{k_\perp^2}\frac{d^2 H_z^{(2,0)}}{dx^2} - \frac{k_y^2}{k_\perp^2} H_z^{(2,0)} = 0. \tag{11}$$

The solution of eq. (11) reads:

$$H_z^{(2,0)} = C_1 \exp(k_y x) + C_2 \exp(-k_y x). \tag{12}$$

The first order correction $H_z^{(2,1)}$ is the solution of the following second order nonuniform differential equation:

$$\frac{1}{k_\perp^2}\frac{d^2 H_z^{(2,1)}}{dx^2} - \frac{k_y^2}{k_\perp^2} H_z^{(2,1)} = \widehat{M} H_z^{(2,0)}. \tag{13}$$

In (13), the r.h.s. reads

$$\widehat{M} H_z^{(2,0)} = -\frac{dH_z^{(2,0)}}{dx}\frac{d}{dx}\left(\frac{1}{k_\perp^2}\right) + H_z^{(2,0)}\left[1 - \frac{d}{dx}\left(\frac{\mu k_y}{k_\perp^2}\right)\right]. \tag{14}$$

The correction $H_z^{(2,1)}$ is found by the method of constant variation:

$$H_z^{(2,1)} = \exp(k_y x)\frac{1}{2k_y}\int_{x_1}^{x}\exp(-k_y x)\,k_\perp^2\widehat{M}H_z^{(2,0)}dx$$
$$-\exp(-k_y x)\frac{1}{2k_y}\int_{x_2}^{x}\exp(k_y x)k_\perp^2\widehat{M}H_z^{(2,0)}dx. \quad (15)$$

Correspondingly, the amplitude of the tangential electric wave field reads

$$E_y^{(2,0)} = \frac{iN_y}{N_\perp^2}\{C_1\exp(k_y x)(1+\mu) -$$
$$C_2\exp(-k_y x)(1-\mu)\}. \quad (16)$$

$$E_y^{(2,1)} = \frac{i}{2kN_\perp^2}\left\{\left[\exp(k_y x)\int_{x_1}^{x}\exp(-k_y x)\,k_\perp^2\widehat{M}H_z^{(2,0)}dx\right.\right.$$
$$\left.+\exp(-k_y x)\int_{x_2}^{x}\exp(k_y x)\,k_\perp^2\widehat{M}H_z^{(2,0)}dx\right]$$
$$+\mu\left[\exp(k_y x)\int_{x_1}^{x}\exp(-k_y x)\,k_\perp^2\widehat{M}H_z^{(2,0)}dx\right.$$
$$\left.\left.-\exp(-k_y x)\int_{x_2}^{x}\exp(k_y x)k_\perp^2\widehat{M}H_z^{(2,0)}dx\right]\right\}. \quad (17)$$

The expression (15) is the correct solution of eq. (13) for arbitrary magnitudes of the constants of integration x_1 and x_2. This makes it possible to choose such magnitudes for the constants $x_{1,2}$ which provide the conditions of applicability of the method of successive approximations, $\left|H_z^{(2,1)}\right| \ll \left|H_z^{(2,0)}\right|$, in the best manner. This consideration results in the following choice:

$$x_1 = (0.5a)sgn(k_y) \text{ and } x_2 = -(0.5a)sgn(k_y). \quad (18)$$

VII. Dispersion relation

A wave field distribution in the form of eqs. (6), (8), (12), and (15) contains four constants of integration: A, B, and $C_{1,2}$. Direct application of the four boundary conditions (continuity of the tangential wave electric and magnetic fields E_y and H_z

at the interfaces $x = -0.5a$ and $x = 0.5a$) can result in derivation of the dispersion relation in the form of a fourth order determinant which could be used for numerical analysis of the problem. However, the boundary conditions $\{H_z\}_{\pm a/2} = 0$ make it possible to exclude the constants A and B:

$$A = C_1 \exp\left(-0.5k_y a\right)(1 + I_1) + \\ + C_2 \exp\left(0.5k_y a\right) + C_2 \exp\left(-0.5k_y a\right) I_2, \quad (19)$$

$$B = C_2 \exp\left(-0.5k_y a\right)(1 + I_4) + \\ + C_1 \exp\left(0.5k_y a\right) + C_1 \exp\left(-0.5k_y a\right) I_3, \quad (20)$$

in the explicit expressions for the boundary conditions $\{E_y\}_{\pm a/2} = 0$. The following notations are used in (19) and (20):

$$I_1 = \int_{-a/2}^{a/2} \frac{k_\perp^2}{2k_y} \left[k_y \frac{d}{dx}\left(\frac{\mu+1}{k_\perp^2}\right) - 1\right] dx, \quad (21)$$

$$I_2 = \int_{-a/2}^{a/2} \frac{k_\perp^2}{2\mathrm{k_y}} \exp(-2k_y x) \left[k_y \frac{d}{dx}\left(\frac{\mu-1}{k_\perp^2}\right) - 1\right] dx, \quad (22)$$

$$I_3 = \int_{-a/2}^{a/2} \frac{k_\perp^2}{2\mathrm{k_y}} \exp(2k_y x) \left[k_y \frac{d}{dx}\left(\frac{1+\mu}{k_\perp^2}\right) - 1\right] dx, \quad (23)$$

$$I_4 = \int_{-a/2}^{a/2} \frac{k_\perp^2}{2k_y} \left[k_y \frac{d}{dx}\left(\frac{\mu-1}{k_\perp^2}\right) - 1\right] dx. \quad (24)$$

At the first glance, the substitution of expressions (19) and (20) into the boundary conditions $\{E_y\}_{\pm a/2} = 0$ has the only consequence to make these conditions more cumbersome. If so, then one has no profit from replacing the dispersion relation in the form of the fourth order determinant by that of the second order, since a computer solves both equations sufficient quickly. However, the elements α_{ij} of the dispersion relation in the form of the second order determinant appear to be of rather simple form after regrouping the *like terms*, which makes the further analytic research of the relation possible. These elements read in the case of positive wavenumber, $k_y > 0$:

$$\alpha_{11} = (1 + I_1)(N_1 - N_y), \tag{25}$$

$$\alpha_{12} = \exp(k_y a)\,(N_y + N_1) + I_2(N_1 - N_y), \tag{26}$$

$$\alpha_{21} = \exp(k_y a)\,(N_3 + N_y) + I_3(N_3 - N_y), \tag{27}$$

$$\alpha_{22} = (1 + I_4)(N_3 - N_y). \tag{28}$$

If SWs propagate in the negative direction, $k_y < 0$, then the elements of the determinant read:

$$\alpha_{11} = (I_1 - 1)(N_3 + N_y), \tag{29}$$

$$\alpha_{12} = \exp(-k_y a)\,(N_y - N_3) + I_2(N_3 + N_y), \tag{30}$$

$$\alpha_{21} = \exp(-k_y a)\,(N_1 - N_y) - I_3(N_1 + N_y), \tag{31}$$

$$\alpha_{22} = (1 - I_4)(N_1 + N_y). \tag{32}$$

For both directions of SW propagation, the term $\alpha_{12}\alpha_{21}$ in the dispersion relation appears to be larger than the term $\alpha_{11}\alpha_{22}$ by the factor of $\exp(2|k_y|a)$. This makes it possible to search for the asymptotic solutions of the dispersion relation as those of the equations

$$\alpha_{12} = 0 \text{ and } \alpha_{21} = 0. \tag{33}$$

If SWs propagate along the y-axis, $k_y > 0$, the eqs. (33) take the following form:

$$\mu_1 N_{\perp 1}^2 = -8N_y^2 \text{ or } \mu_3 N_{\perp 3}^2 = 8N_y^2. \tag{34}$$

If SWs propagate in the opposite direction, $k_y < 0$, then the eqs. (33) take a similar but different form:

$$\mu_3 N_{\perp 3}^2 = -8N_y^2 \text{ or } \mu_1 N_{\perp 1}^2 = 8N_y^2. \tag{35}$$

Implying the condition (10) of applicability of the present approach suggests to search for the solutions of eqs. (34) and (35) nearby the hybrid frequencies, where $|\mu_{1,3}| \gg 1$. This circumstance explains why SWs do not propagate along the interface between isotropic plasmas, in which case $\mu_{1,3} \equiv 0$. Consequently, the present paper does not contradict with the conclusions of Romanov [9] who

considered isotropic plasma and proved the absence of any solutions of the corresponding dispersion relation in the case of short wavelengths, $|k_y|a \gg 1$.

Note that the condition (10) also fails nearby the hybrid frequencies. After substituting the expression for $\varepsilon_1 = \pm(|\varepsilon_2^3|/(8N_y^2))$, which follows from the dispersion relations (34) and (35), into strong inequality (10) one derives the following restrictions on the wavenumber in the lower hybrid range, $\omega \approx \omega_{LH}$ (here $\omega_{LH} = [(|\omega_e|\omega_i)^{-1} + \Omega_i^{-2}]^{-\frac{1}{2}}$ is the lower hybrid frequency):

$$|k_y|\delta \gg \left(\frac{64m_e}{m_i}\frac{Z^2}{1+Z^2}\right)^{\frac{1}{4}}, \tag{36}$$

and in upper hybrid range, $\omega \approx \omega_{UH}$ (here $\omega_{UH} = (\Omega_e^2 + \omega_e^2)^{\frac{1}{2}}$ is the upper hybrid frequency):

$$|k_y|\delta \gg \left(64\frac{Z^2+1}{Z^4}\right)^{\frac{1}{4}}, \tag{37}$$

which also can be treated as consideration of short wavelength SWs. Hereinafter, $\delta = c/\Omega_\mathrm{e}$ is the skin-depth and $Z \equiv \Omega_e/|\omega_e|$ is the ratio of electron plasma and electron cyclotron frequencies.

Since $|\mu_{1,3}| \gg 1$ in the range of hybrid frequencies, the expression for $N_{\perp 1,3}^2$ can be further simplified to $N_\perp^2 \approx \varepsilon_2^2/\varepsilon_1$. Then the dispersion relations (34) and (35) read

$$\varepsilon_{21}^3/\varepsilon_{11}^2 = 8N_y^2 \text{ or } \varepsilon_{23}^3/\varepsilon_{13}^2 = -8N_y^2 \text{ if } k_y > 0, \tag{38}$$

$$\varepsilon_{23}^3/\varepsilon_{13}^2 = 8N_y^2 \text{ or } \varepsilon_{21}^3/\varepsilon_{11}^2 = -8N_y^2 \text{ if } k_y < 0. \tag{39}$$

At this step, one can expect to find eight solutions of the four dispersion relations (38) and (39) – two for each equation (one of the solutions is expected in the lower hybrid frequency range, and the other – in the upper hybrid frequency range). However, the existence of these solutions depends on the sign of the

permittivity tensor component ε_2. In the range of the lower hybrid frequency, $\omega \approx \omega_{LH1,2}$, the permittivity tensor component ε_2 is negative:

$$\varepsilon_2 = -\frac{\Omega_e^2}{|\omega_e|\omega_{LH}} < 0. \quad (40)$$

This means that only α_{21} can turn to zero and $\alpha_{12} \neq 0$ in the lower hybrid frequency range:

$$\varepsilon_{23}^3/\varepsilon_{13}^2 = -8N_y^2, \text{ if } k_y > 0, \text{ and } \varepsilon_{21}^3/\varepsilon_{11}^2 = -8N_y^2, \text{ if } k_y < 0. \quad (41)$$

In the upper hybrid frequency range, $\omega \approx \omega_{UH1,3}$, the permittivity tensor component ε_2 is positive:

$$\varepsilon_2 = \frac{|\omega_e|}{\omega_{UH}} > 0. \quad (42)$$

This makes it possible to narrow our search to the consideration of the equation $\alpha_{12} = 0$, while $\alpha_{21} \neq 0$:

$$\varepsilon_{21}^3/\varepsilon_{11}^2 = 8N_y^2, \text{ if } k_y > 0, \text{ and } \varepsilon_{23}^3/\varepsilon_{13}^2 = 8N_y^2, \text{ if } k_y < 0. \quad (43)$$

When the model under the consideration was described in Section II, the symmetry of the three-component plasma structure was stressed. This symmetry can be seen in eqs. (41) and (43). Specifically, the replacement of the wavenumber sign, $k_y \leftrightarrow -k_y$, is accompanied by replacement of the magnitudes of the plasma particle density, $\varepsilon_{21} \leftrightarrow \varepsilon_{23}$ and $\varepsilon_{11} \leftrightarrow \varepsilon_{13}$, in these dispersion relations.

VIII. Numerical analysis of the dispersion relation

The dispersion curves are shown in Figs. 2-4 in the form of the wave eigenfrequency ω dependence on the wavenumber k_y. During the calculations the plasma particle density within the transition layer is assumed to vary linearly,

$$n(x) = n_1 + (n_3 - n_1)(x + 0.5a)/a, \quad (44)$$

and the assumptions are checked up, under which the dispersion relation is derived. In particular, the correction $H_z^{(1)}$ to the amplitude of the longitudinal magnetic wave field is small in absolute value as compared to the main term $H_z^{(0)}$, as well as $|k_y|a \gg 1$.

All the Figs. 2-4 are presented as the dependence of normalized SW eigenfrequencies on the normalized wavenumber $k_y\delta_1$. The subscript "1" means that the plasma particle density of the left uniform half space is applied. The latter choice is explained by the following reason. The dispersion properties of surface type electromagnetic waves propagating along the azimuthal angle in circular metal waveguides entirely filled by two layers of plasma in axial static magnetic field were studied in [24]. The wave dispersion properties were found to depend mostly on the electrodynamic characteristics of the medium with smaller plasma particle density. Electrodynamic properties of the plasma with larger density were reported to introduce only small corrections to eigenfrequency and spatial wave field distribution.

The ratio of the electron to ion masses is chosen in the calculations to be as in deuterium, $m_e/m_i \approx 2.69 \times 10^{-4}$. Since the order of hybrid frequencies, $\omega_{LH1} < \omega_{LH3} < \omega_{UH1} < \omega_{UH3}$, is clear without specific explanation, the branches are normalized in Figs. 2-4 by these hybrid frequencies, respectively.

The existence of eight branches of the dispersion curves is demonstrated in Fig. 2 by solid curves. The plasma particle density of the right uniform plasma half space is assumed to be higher than that of the left half space by the factor of ten, $n_3/n_1 = 10$. The magnitude of the external static magnetic field is taken into account via the ratio of electron plasma and electron cyclotron frequencies Z. Since the calculations for the Figs. 2,3 are carried out on the base of eqs. (41) and (43), which do not contain the transition layer width a because they are derived in the

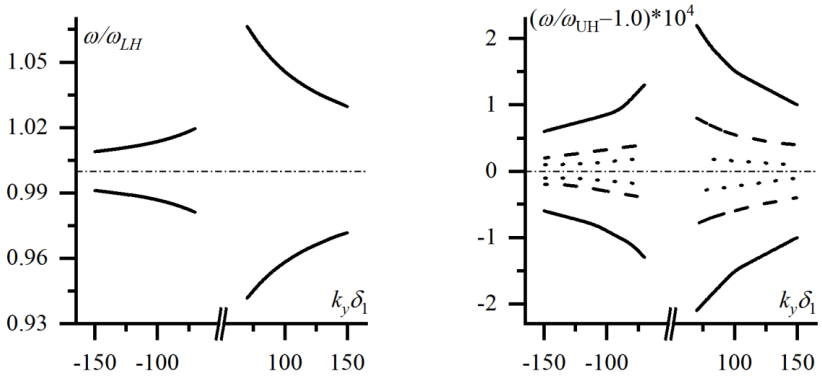

Fig 2. SW eigenfrequency ω/ω_{LH} vs the wavenumber subject to the magnitude of an external static magnetic field. Left (lower hybrid SWs): ω/ω_{LH1} for $k_y < 0$, and ω/ω_{LH3} for $k_y > 0$ (according to eq. (44)). Right (upper hybrid SWs): ω/ω_{UH3} for $k_y < 0$, and ω/ω_{UH1} for $k_y > 0$ (according to eq. (46)); $Z_1 \equiv \Omega_{e1}/|\omega_e| = 5.0$ (solid curves), $Z_1 \equiv \Omega_{e1}/|\omega_e| = 10.0$ (dashed curves), $Z_1 \equiv \Omega_{e1}/|\omega_e| = 20.0$ (dotted curves)

limit $|k_y|a \to \infty$, then the magnitude of a is not specified for these figures. One can see in Fig. 2 (right) that smaller strength of the external static magnetic field B_0 (which is equivalent to higher magnitudes of Z) causes a smaller difference between the SW eigenfrequencies and the upper hybrid frequency. This is true for both relative, $|(\omega - \omega_{UH})/\omega_{UH}|$, and absolute, $|\omega - \omega_{UH}|$, difference. This observation is in line with the conclusion of the present paper that the short wavelength SWs considered here can propagate in magnetized plasma only. The same decrease of B_0 by the factor of four causes negligible effect (maximum 0.042%) on the eigenfrequency of lower hybrid SWs in Fig. 2 (left). That is why neither dashed nor dotted curves are present there.

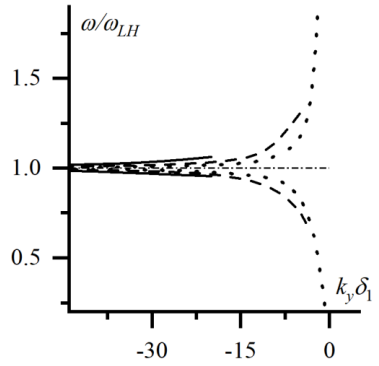

Fig 3. SW eigenfrequency ω/ω_{LH} vs the wavenumber subject to the transition layer width. $\omega/\omega_{LH1} < 1.0$, and $\omega/\omega_{LH3} > 1.0$. $Z_1 = 5.0$. $a/\delta_1 = 0.3$ (solid curves), $a/\delta_1 = 1.0$ (dashed curves), $a/\delta_1 = 3.0$ (dotted curves)

It is clear that the considered SWs cannot exist in the limiting case of zero plasma particle density gradient, $(n_3 - n_1)/a = 0$. This limiting case can be realized either by increasing of transition layer width a as compared to the skin-depth δ_1 which is realized in Fig. 3 or by decreasing the ratio of plasma particle density in the right and left uniform half spaces, n_3/n_1, which is presented in Fig. 4. The results shown in Figs. 3,4 are obtained via calculating the full dispersion relation (29)-(32).

Increase of the transition layer width a is demonstrated in Fig. 3 to manifest itself in three ways. First, the larger a is, the smaller the magnitude of $|k_y|$ can be taken to remain in the framework of the assumption $|k_y|a \gg 1$. Second, increase of a is accompanied by a decrease of the difference between the SW eigenfrequency and the correspondent hybrid frequency, $|\omega - \omega_{LH}|$, for fixed magnitude of the wavenumber. It is the latter phenomenon which is treated in the present paper as disappearance of SWs with turning of the plasma particle density gradient to zero. This result is in qualitative agreement with the conclusion of the paper [24], where the SW disappearance in the case of a sharp interface of two plasma layers in circular waveguides was investigated. Third, the larger a is, the larger the difference $|\omega - \omega_{LH}|$ is observed for smallest possible magnitude of $|k_y|$.

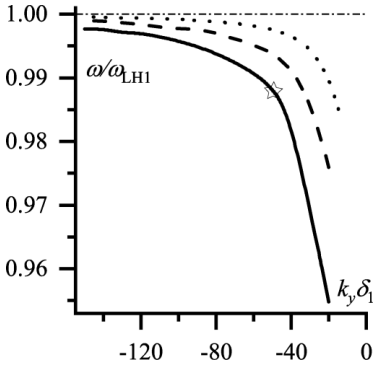

Fig 4. SW eigenfrequency ω/ω_{LH} vs the wavenumber subject to the difference in plasma particle density in left and right half spaces, n_3/n_1. $n_3/n_1 = 10.0$ (solid curve), $n_3/n_1 = 3.0$ (dashed curve), $n_3/n_1 = 1.25$ (dotted curve). $a/\delta_1 = 0.3$, $Z_1 = 5.0$

Decrease of the ratio n_3/n_1 is also shown in Fig. 4 to cause the SW disappearance. Lower hybrid SWs are inspected as example. The smaller the ratio n_3/n_1 is, the smaller the difference $|\omega - \omega_{LH1}|$ is. Here one should emphasize the applicability of the initial assumptions made in the present research. The choice of the smallest magnitudes of $|k_y|$ to be applied in the calculations is determined by the necessity to provide these assumptions. Specifically, $\min\{|k_y|\delta_1\} = 20.0$ in Fig. 4 provides $|k_y|a = 6.0 \gg 1$. The precision of application of the method of successive approximations is worse for smaller magnitudes of $|k_y|\delta_1$. In particular, for $|k_y|\delta_1 = 20.0$, the precision of application of the method of successive approximations is about 35% for $n_3/n_1 = 10.0$ (solid curve), 20% for $n_3/n_1 = 3.0$ (dashed curve), and 8% for $n_3/n_1 = 1.25$ (dotted curve). The precision is much better ($|H_z^{(1)}/H_z^{(0)}|$<0.1%) already for $|k_y|\delta_1 = 40.0$.

In the following, the possibility of experimental observation of the phenomenon reported in the present paper is demonstrated. The results presented in Fig. 4 are chosen for example, within which $Z_1 = 5.0$ and $a = 0.3\delta_1$. If the structure with moderate plasma particle density, $n_1 \approx 10^{11}\ cm^{-3}$, is considered, then the magnetic field B_0 should be of $\approx 203\ G$; and the transition layer width should be of $\approx 0.5\ cm$.

If to choose the abscissa magnitude as $|k_y|\delta_1 = 50.0$ (the corresponding point is marked in Fig. 4 by the star), then the wavenumber is $|k_y| \approx 30\ cm^{-1}$. In this case, the wave eigenfrequency is smaller than the lower hybrid frequency $\omega_{LH1} \approx 57.5 \times 10^6\ s^{-1}$ by $\approx 0.668 \times 10^6\ s^{-1}$.

To complete the presentation of numerical results the wave amplitude distribution in the vicinity of the transition layer is displayed in Fig. 5. The distribution is calculated for the same conditions as those related to the star in Fig. 4. Absolute values of the two amplitudes are shown in Fig. 5 - those of the longitudinal magnetic wave field, $|H_z(x)|$, and transversal electric wave field, $|E_y(x)|$. The maximum of the amplitudes is situated near the interface $x = -0.5a$ rather than at $x = 0.5a$. This is in agreement with the choice of the frequency which is a little bit smaller than ω_{LH1}. The amplitudes are displaced in arbitrary units, and maximum magnitude of $|E_y(x)|$ is chosen to be the unit. The maximum amplitude of $|H_z(x)|$ is chosen on Fig. 5 to be equal to 0.5 with the goal to make visible the difference and/or similarity in the spatial distribution of the two amplitudes. However, in the calculations, $Max\{|E_y(x)|\} \approx 10.0 Max\{|H_z(x)|\}$. Similar radial profiles of the surface wave electromagnetic fields peaked nearby the plasma-plasma circular interface were presented in [24]. Within uniform plasmas, the amplitudes of the wave fields are proportional to each other: $|E_y(x)| \approx 10.0|H_z(x)|$ in the left uniform plasma, $x < -0.5a$; and $|E_y(x)| \approx |H_z(x)|$ in the right uniform plasma, $x > 0.5a$. Consequently, within the transition layer, the amplitude $|H_z(x)|$ decreases more smoothly than $|E_y(x)|$. Specifically, the amplitude $|E_y(x)|$ deceases twice at the distance of $\approx 0.072a$ from the interface $x = -0.5a$, while the amplitude $|H_z(x)|$ – at the distance of $\approx 0.12a$.

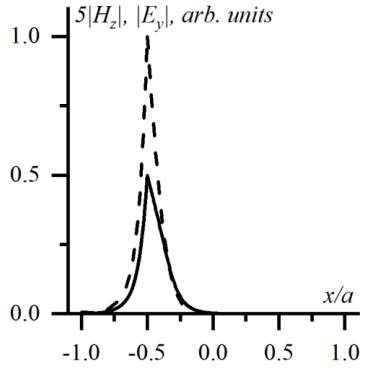

Fig 5. Absolute magnitude of SW field amplitudes, $|E_y(x)|$ (dashed curve) and $|H_z(x)|$ (solid curve), vs the x-coordinate. $n_3/n_1 = 10.0$, $a/\delta_1 = 0.3$, $Z_1 = 5.0$, $k_y\delta_1 = -50.0$, $\omega \approx 0.01591|\omega_e|$

IX. Conclusions and discussions

Short wavelength electromagnetic waves of surface nature are shown to propagate along the slab transition layer between two uniform plasma half-spaces in Voigt geometry in the lower and higher hybrid frequency ranges. In this case, the wave penetration depths into the plasmas are of the order of the inverse wavenumber, $k_{1,3} \approx |k_y|$. Asymptotic methods are applied to determine the wave field spatial distribution within the transition layer. The transition layer width is assumed to be large as compared with the wavelength. Due to this assumption, the results of the present paper cannot be compared with those in the case of a sharp interface between the two uniform half spaces.

Here, the influence of the transition layer width as compared with the plasma skin-depth on the wave dispersion properties is studied. Disappearance of the surface waves with decreasing plasma particle density gradient within the transition layer is shown to manifest itself by decreasing the difference between the wave eigenfrequency and corresponding hybrid frequency. The plasma particle density gradient within the transition layer is determined by the layer width a and difference

between the two densities of the uniform plasma half-spaces $|n_3 - n_1|$. Increase of a and decrease of the difference $|n_3 - n_1|$ are shown to cause a qualitatively similar influence on the wave dispersion properties by pushing the dispersion curve to the corresponding hybrid frequencies.

The contradiction between the results obtained in the present paper with those reported by Romanov [9] are explained as follows. A simple and clear from the physical point of view criterion was suggested in [9] for switching on/off the possibility for SWs to propagate along the transition layer between two isotropic ($B_0 = 0$) plasma half spaces. The SWs were demonstrated to disappear in the limit of sufficiently large transition layer width a as compared with the wavelength $2\pi/|k_y|$. In this case, $|k_y|a \gg 1$, and the dispersion relation derived in [9] for isotropic plasmas was analytically demonstrated to have no roots. Application of an external static magnetic field B_0 is the necessary condition for the short wavelength SW propagation in Voigt geometry. The presented results become meaningless in the case of isotropic plasmas with $B_0 = 0$.

Note that the possibility of SW propagation with sufficiently high wavenumber, $|k_y| > 1/a$, in Voigt geometry along the transition layer between a plasma half space and a metal was demonstrated as well in [20]. There, the figures, displaying the dependence of SW eigenfrequency on the transverse wavenumber normalized by the transition layer width $|k_y|a$, with abscissa up to ≈ 7.5 were given. No problems with solving the dispersion relation for larger products $|k_y|a$ were reported.

Unfortunately, the conclusions above cannot be considered as universal. First, they relate to electromagnetic surface wave propagation perpendicular to the static magnetic field ($k_z = 0$). This assumption significantly simplifies the derivation of the dispersion relation, since it provides separation of electromagnetic waves into ordinary polarized and extraordinary polarized modes. In addition, just extraordinary

polarized modes are studied here. Note that ordinary polarized waves cannot be of surface nature in this case. Second, the approximation of sufficiently short transversal wavelengths is applied to get use of the asymptotic method to solve Maxwell equations within the transition layer. Third, a slab geometry is considered. On the other hand, the applied method does not imply any direct restrictions on the width of the transition layer as compared to the skin-depth $\delta = c/\Omega_e$.

The presented results can be applied, e.g., in plasma electronics, plasma-antenna systems, plasma production, nano-technologies, and for explanation of electromagnetic wave propagation in the plasma periphery of magnetic confinement fusion devices.

The data that supports the findings of this study are available within the article.

Acknowledgement

This work is partially supported by the Ministry of Education and Science of Ukraine Research Grant 0123U101904.

References

1. I. Girka, and M. Thumm, Surface Flute Waves in Plasmas (Springer, Cham, 2022). https://doi.org/10.1007/978-3-030-98210-2_1

2. M. Thumm, "State-of-the-art of high-power gyro-devices and free electron masers," J. Infrared Milli Terahz Waves, **41**, 1–140 (2020). https://doi.org/10.1007/s10762-019-00631-y

3. S. Sun, Q. He, S. Xiao, Q. Xu, X. Li and L. Zhou, "Gradient-index meta-surfaces as a bridge linking propagating waves and surface waves," Nature Materials, **11**, 426–431 (2012). https://doi.org/10.1038/nmat3292

4. J. Langer, D. Jimenez de Aberasturi, J. Aizpurua, R. A. Alvarez-Puebla, B. Auguié, J. J. Baumberg, G. C. Bazan, S. E. J. Bell, A. Boisen, A. G. Brolo, et al.,

"Present and future of surface-enhanced Raman scattering," ACS Nano, **14**, No. 1, 28–117 (2020). https://doi.org/10.1021/acsnano.9b04224

5. T. Anderson, Plasma Antennas (Artech House, Boston, 2020).

6. I. Zhelyazkov, and V. Atanassov, "Axial structure of low-pressure high-frequency discharges sustained by travelling electromagnetic surface waves," Physics Reports, **255**, 79-201 (1995). https://doi.org/10.1016/0370-1573(94)00092-H

7. R. R. Weynants, "ICRF review: From ERASMUS to ITER," Proceedings of AIP Conference on Radio Frequency Power in Plasmas, **1187**, 3-12 (2009). https://doi.org/10.1063/1.3273778

8. A. Messiaen, and V. Maquet, "Coaxial and surface mode excitation by an ICRF antenna in large machines like DEMO and ITER," Nuclear Fusion, **60**, No. 7, 07601 (2020). https://doi.org/10.1088/1741-4326/ab8d05

9. Yu. A. Romanov, "Theory of characteristic losses in thin films," Soviet Physics JETP, **20**, No. 6, 1424-1432 (1965).

10. K. N. Stepanov, "Concerning the effect of plasma resonance on surface wave propagation in a nonuniform plasma," Soviet Physics – Technical Physics, **10**, No. 6, 773-780 (1965).

11. J V. Hollweg, "Resonance absorption of magnetohydrodynamic (MHD) surface waves - viscous effects," The Astrophysical Journal, **320**, 875-883 (1987). https://doi.org/10.1086/165604

12. Yu. M. Aliev, and G. Brodin, "Instability of a strongly inhomogeneous plasma," Physical Review A, **42**, issue 4, 2374-2378 (1990). https://doi:10.1103/PhysRevA.42.2374

13. J. Lundberg, "Nonlinear surface waves in a strongly inhomogeneous plasma," Contributions to Plasma Physics, **33**, Issue 2, 89-95 (1993). https://doi.org/10.1002/ctpp.2150330203

14. G. Brodin, and J. Lundberg, "Nonlinear surface waves in a plasma with a diffuse boundary," Physics of Plasmas, **1**, Issue 1, 96 (1994). https://doi.org/10.1063/1.870465

15. L. L. Alves, S. Letout, and C. Boisse-Laporte, "Modeling of surface-wave discharges with cylindrical symmetry," Physical Review E, **79**, 016403, (2009). https://doi.org/10.1103/PhysRevE.79.016403

16. I. P. Ganachev, and H. Sugai, "Production and control of planar microwave plasmas for materials processing," Plasma Sources Science and Technology, **11**, No. 3A, A178 (2002). https://doi.org/10.1088/0963-0252/11/3A/327

17. I. A. Girka, V. I. Lapshin, and K. N. Stepanov, "Plasma heating near satellite Alfven resonances in stellarators," Plasma Physics Reports, **23**, No. 1, 19-27 (1997)

18. I. O. Girka, "Resonant influence of bumpy steady magnetic field ripples on the structure of the local Alfven resonance," Contributions to Plasma Physics, **41**, No. 1, 33-44 (2001). https://doi.org/10.1002/1521-3986(200101)41:1<33::AID-CTPP33>3.0.CO;2-9

19. V. O. Girka, and I. O. Girka, "Additional ECR heating of a radially inhomogeneous plasma via the absorption of satellite harmonics of the surface flute modes in a rippled magnetic field," Plasma Physics Reports, **32**, No. 12, 1047-1051 (2006). https://doi.org/10.1134/S1063780X06120075

20. N. A. Azarenkov, A. N. Kondratenko, V. N. Melnik, and V. P. Olefir, "Surface waves at a plasma-metal interface propagating transverse to a magnetic field," Radiotekh. Elektron., **30**, 2195-2201 (1985). In Russian.

21. N. A. Azarenkov, and K. N. Ostrikov, "Surface magnetoplasma waves at the interface between a plasma-like medium and a metal in a Voigt geometry," Physics Reports, **308**, 333–428 (1999). https://doi.org/10.1016/S0370-1573(98)00032-5

22. W. Tierens, L. Colas, and EUROfusion MST1 Team, "Slab-geometry surface waves on steep gradients and the origin of related numerical issues in a variety of

ICRF codes," Journal of Plasma Physics, **87**, No. 4, 905870405 (2021). https://doi.org/10.1017/S002237782100074X

23. N. A. Azarenkov, A. N. Kondratenko, and V. V. Kostenko, "Skew MHD surface waves at a plasma-metal boundary," Soviet Technical Physics, **32**, No. 3, 360-361 (1987).

24. I. Girka, R. Bilato, and W. Tierens, "Azimuthal surface waves in circular metal waveguides entirely filled by two layers of plasma in axial static magnetic field," Physics of Plasmas, **30**, No. 2, 022109 (2023). https://doi.org/10.1063/5.0134049

Physics of Plasmas

PLEASE CITE THIS ARTICLE AS DOI: 10.1063/5.0165416

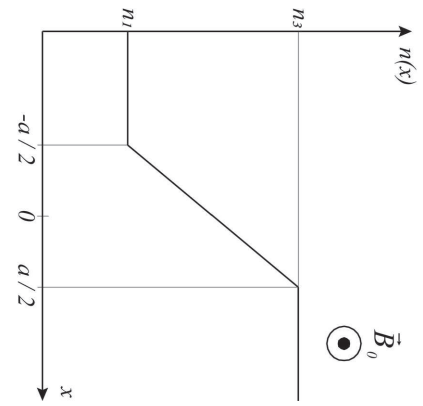

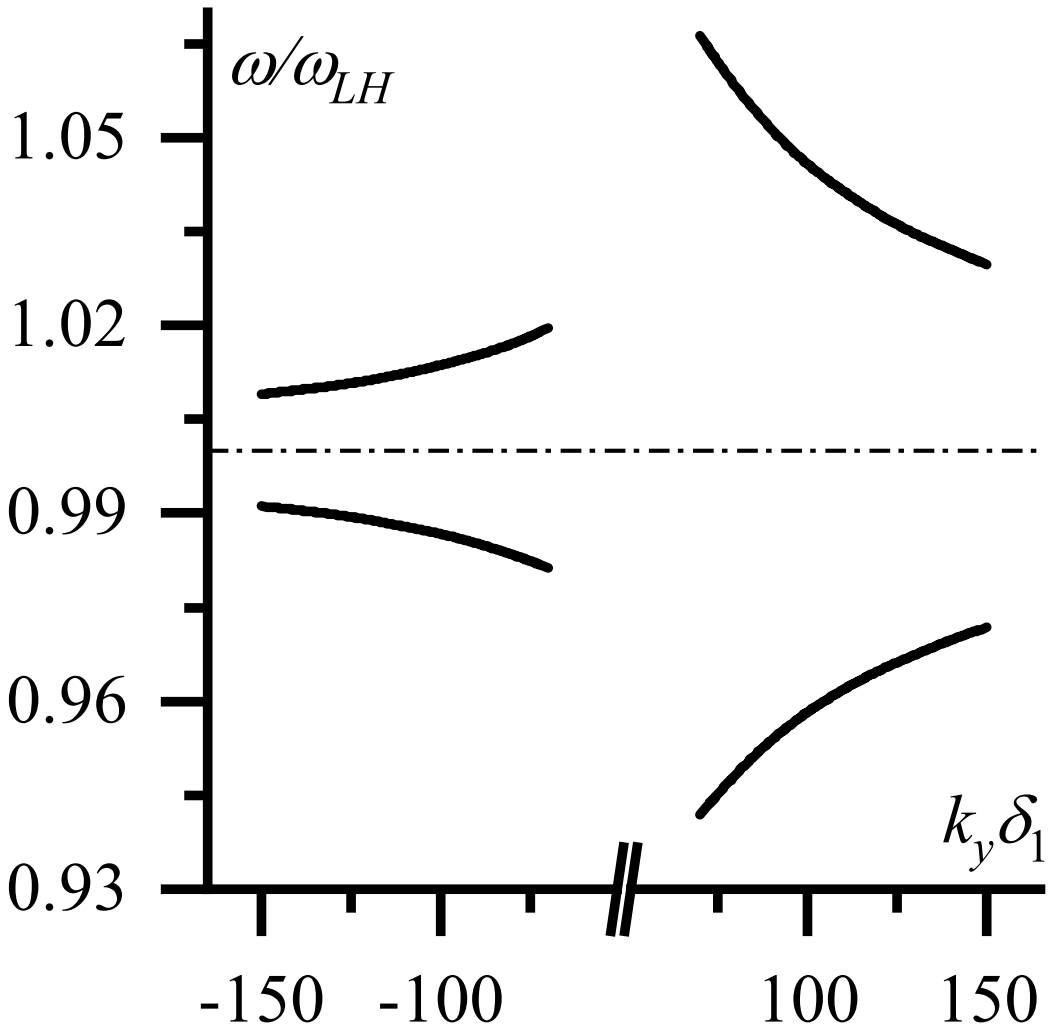

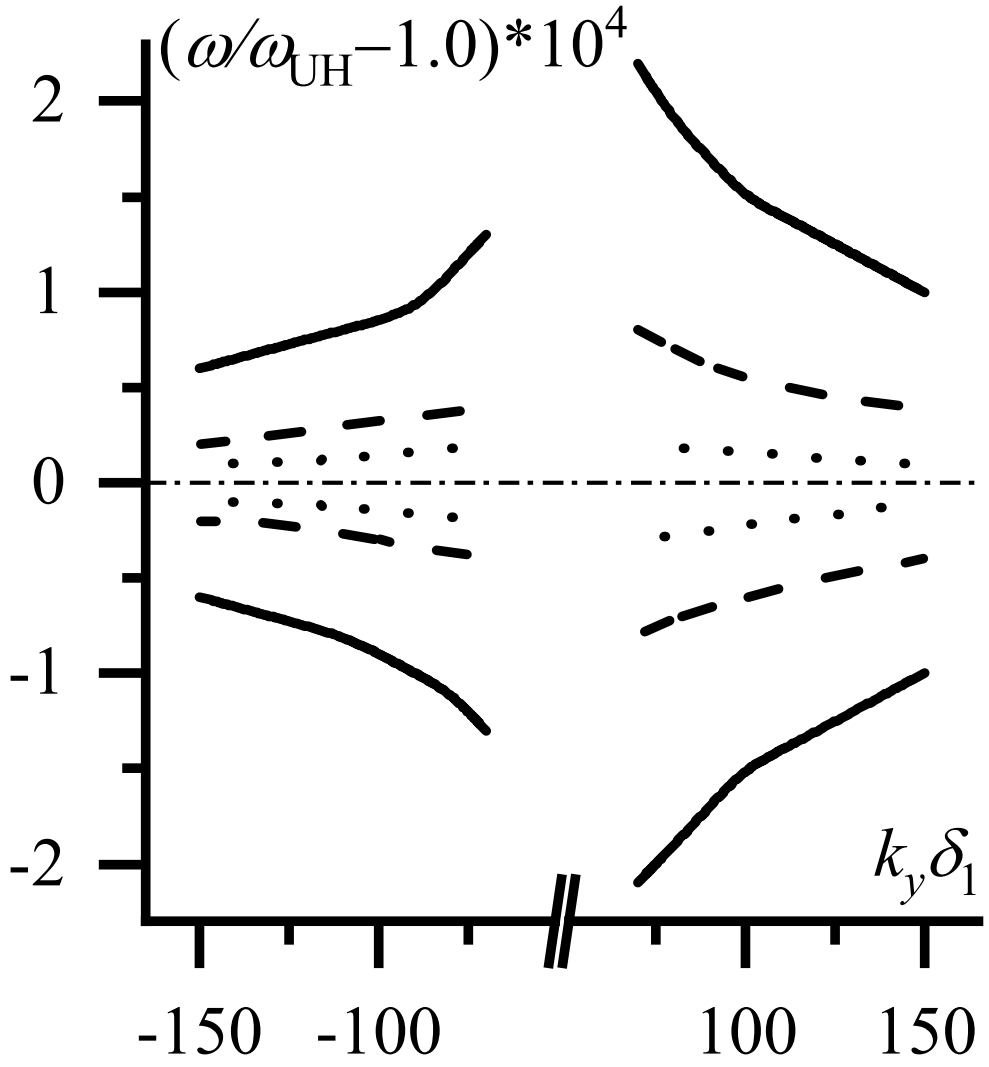

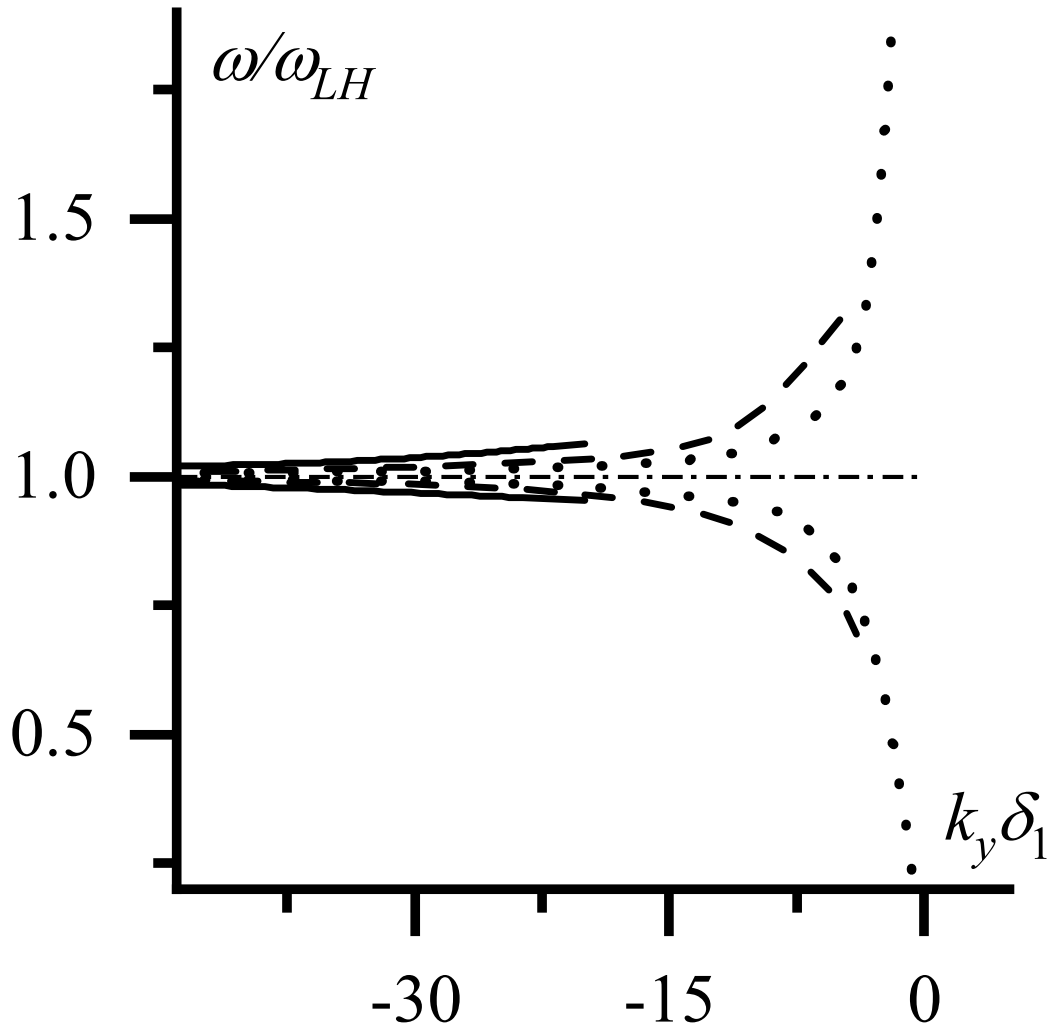

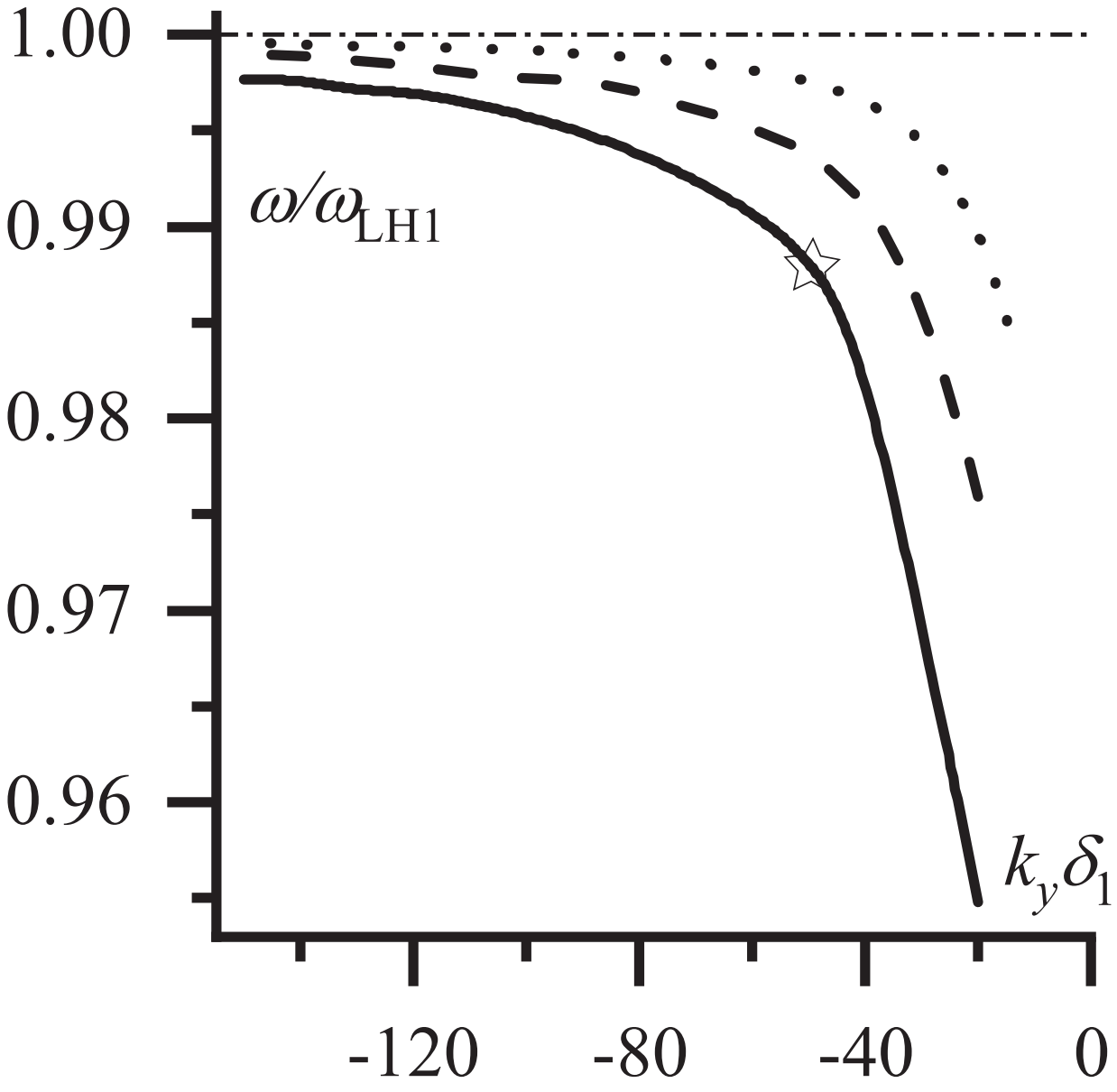

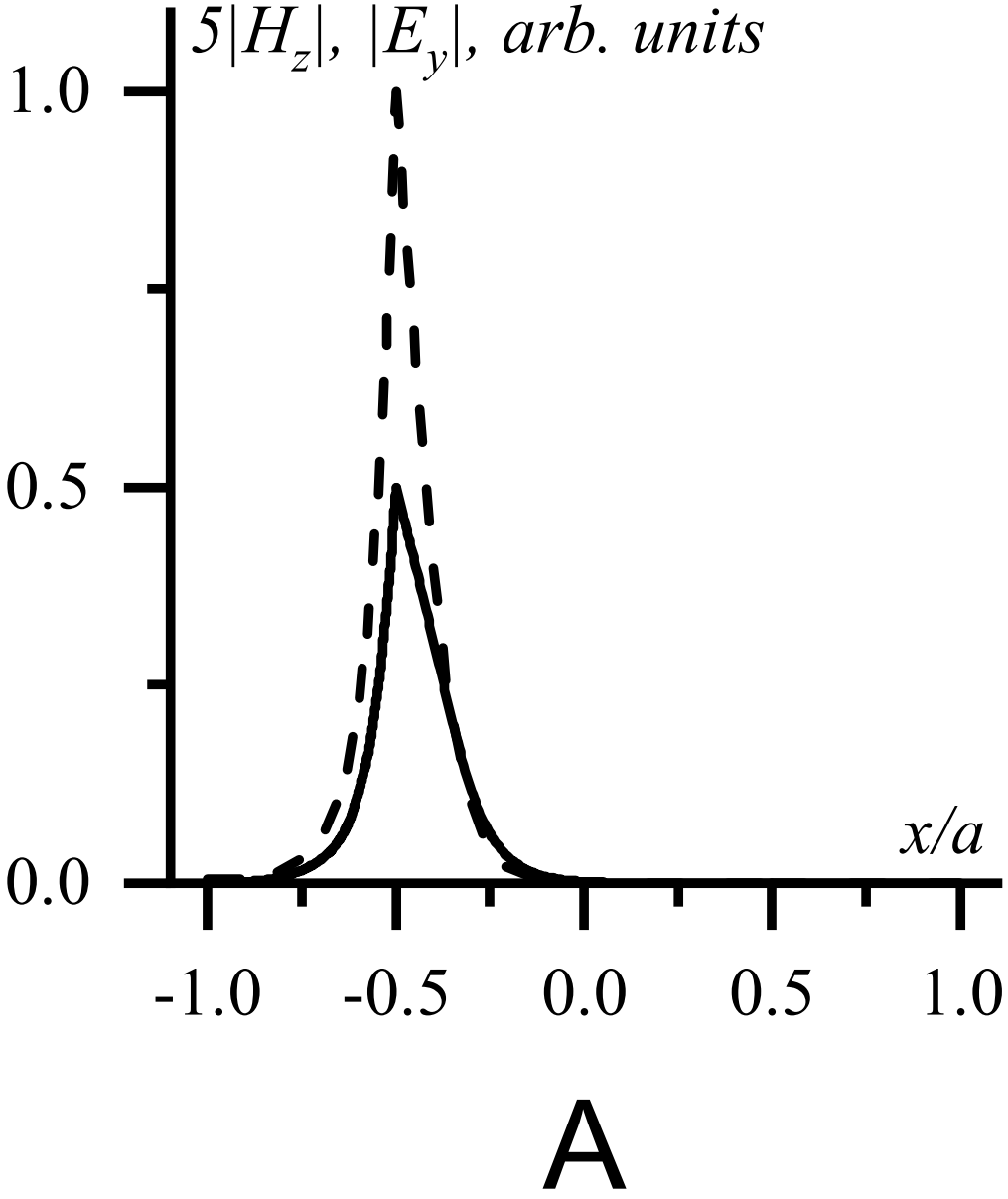

A